

Available online at www.sciencedirect.com**SciVerse ScienceDirect**

Procedia Environmental Sciences 18 (2013) 366 – 371

Procedia

Environmental Sciences

2013 International Symposium on Environmental Science and Technology (2013 ISEST)

Effect of morphology and pore structure of SBA-15 on toluene dynamic adsorption/desorption performance

Yuan Qin, Yi Wang, Huiqiong Wang, Jinsuo Gao, Zhenping Qu*

Key Laboratory of Industrial Ecology and Environmental Engineering (MOE), School of Environmental Science and Technology, Dalian University of Technology, Dalian 116024, China

Abstract

The dynamic adsorption/desorption behavior of VOCs (C_7H_8) was evaluated for mesoporous SBA-15 silicas with four kinds of morphologies and pore sizes on a fixed bed unit. The SBA-15 silica with interconnected rodlike morphology exhibited exceptionally good breakthrough behavior, a higher adsorption capacity, and better desorption performance for toluene. The large dynamic VOC capacity of the interconnected rodlike silica was attributed to the pore system of the micropores and mesopore size, group-togethering rods which can aggregate to enhance the ability of adsorption, together with the smoother surface.

© 2013 The Authors. Published by Elsevier B.V. Open access under [CC BY-NC-ND license](http://creativecommons.org/licenses/by-nc-nd/3.0/).
Selection and peer-review under responsibility of Beijing Institute of Technology.

Key words: SBA-15; Morphology; Pore structure; VOCs; Dynamic sorption

1. Introduction

VOCs are known as one of the major contributors to the greenhouse effect, ozone layer depletion, the formation of photochemical smog and secondary organic aerosol (SOA) [1,2]. It is very necessary to find an environmental-friendly way minimizing the release of VOCs into the atmosphere. Among a number of available technologies, adsorption is attractive for its flexibility of the system, low energy and cheap operation costs [3,4]. Recent researches have shown that the SBA-type material with bimodal pore distribution shows a high affinity for various VOCs due to their complementary micropores [5-7]. A variety of SBA-15 materials morphologies such as fiberlike, rod, sphere, platelet, gyroid, discoid, sausage and doughnut can be obtained by changing the synthetic parameters [8-10]. As is reported, these different external morphologies of SBA-15 materials can influence their sorption behaviours [11,12]. In the process of adsorbents development, morphological study at the micrometer level in mesoporous silicas is

* Corresponding author. Tel.: 15542663636
E-mail address: quzhenping@dlut.edu.cn

still a significant factor in helping to control emission of VOCs. Simple morphologies with short, unhindered path lengths such as small spheres and crystal-like particles as well as short, straight rods are also beneficial for applications. But it is still not very clear about the effect of different morphologies of mesoporous SBA-15 materials on the adsorption/desorption behaviors. Additionally, there has been no successful research about the application in sorption behaviors of special “bimodal pore system” and morphologies of mesoporous SBA-15. Thus the comparison of the sorption behaviors among different meso- and microstructures of SBA-15 materials with similar textural properties would be very meaningful for further studying the VOCs sorption behavior on mesoporous materials. In our research, four kinds of morphologies of SBA-15 materials with “bimodal pore system” were synthesized, and the ability of different SBA-15 silicon on toluene sorption was compared and the association between their meso-/microstructures and toluene sorption was discussed.

2. Experimental Section

2.1. Synthesis

Mesoporous SBA-15 silicas were synthesized using triblock copolymer Pluronic P123 (EO20PO70EO20) as the template and tetraethylorthosilicate (TEOS) as the silicate source under acidic conditions. In a typical synthesis, 4.0 g of P123 was added to 120 mL of 2 M HCl and stirred at 40°C for 4 h, then, 8.50 g TEOS was added. After 5 min of vigorous stirring, the mixture was kept under static condition at 40°C for 20 h, followed by 24 h at different temperatures (60°C and 100°C). The sample was assigned as A and B, respectively. Another sample C was synthesized only under the first static period (40°C for 20 h). The fourth SBA-15 sample (D) was synthesized in a conventional way: the mixture above mentioned was transferred into Teflon reaction container and kept it at 100°C for 2 days. All the solid products were collected by filtration, washed with water, dried at 100°C for 24 h, and calcined at 540°C.

2.2. Characterization

Powder X-ray diffraction (XRD) patterns were obtained with a Rigaku Rotaflex diffractometer equipped with a rotating anode using Cu K α Radiation. Nitrogen sorption experiments were performed at 77 K on a NOVA 4200e surface area and pore size analyzer. The Brumauer–Emmett–Teller (BET) method was utilized to calculate specific surface areas. Pore size distributions were derived from the adsorption branches using the Barrett–Joyner–Halanda (BJH) method. SEM was performed on a JEOL JSM-6360 scanning electron microscope operating at an acceleration voltage of 20–30 kV.

2.3. Toluene adsorption

120 mg of pelletized samples were loaded in the adsorption bed and heated at 300°C for 30 min under Ar atmosphere. Air was taken and adjusted to keep the total gas flow rate at 55 ml/min. The adsorption capacity was evaluated from breakthrough curves obtained at 25°C in a mixed gas flow. Then the samples were purged with air for a period time until the concentration was low enough (less than 5% of original C₇H₈ concentration). Following the saturation adsorption, as indicated by the stable signals of toluene in the GC and mass spectrometer, the reactor was purged with pure He for 1 h. For the desorption experiment, He was passed through the reactor by ramping the temperature from RT to 400°C at a heating rate of 10°C/min and a flow rate of 50 mL/min. VOCs concentrations of the inlet and outlet were analyzed by gas chromatography (GC).

3. Results and discussion

3.1. Characterization

Scanning electron microscopy (SEM) images of the SBA-15 silicas are shown in Fig. 1. Sample A shows small particles (ca. 800 nm in diameter) with uniform morphology. And every small particle is a smooth hexagonal platelet with very short length in long axis direction. Sample B exhibits compact and rough rodlike particle morphology and the size is about 1 μm length and 0.5 μm width. Sample C consists of a large number of rodlike particles ca. 1 μm length and 0.5 μm width. These particles have a great tendency to group together and form long constituents. Sample D shows the fiberlike morphology and the length of the fibers can reach long (20-30 μm).

Fig. 2. (a) shows the X-ray diffraction patterns of mesoporous A, B, C and D SBA-15 samples. The diffraction intensity of the three peaks for sample A and C are well-resolved peaks in the range of $2\theta=0.8-2\theta$. The peaks on sample B and D can be indexed as the (100), (110), (200) reflections of the 2D hexagonal ordering in the $p6mm$ space group hexagonal space [13]. For sample A-C, it is found that the position of the (100) peak obviously shifts to higher 2θ values due to the smaller mesopore size compared with D and the intensity of all peaks differs which indicates the order degree of the mesostructures. The nitrogen sorption isotherms of all samples show type IV sorption isotherm with an H1-type hysteresis loop at a relative pressure extent of 0.4-1.0, which is characteristic of the mesoporous materials with 1D cylindrical channels in a hexagonal arrangement (Fig. 2b). The structure properties of different samples prepared are collected in Table 1. The pore size of the samples ranges from 3.82 nm to 7.72 nm. All samples show an ordered array of cylindrical 1D channels and it is composed of numbers of micropores stacked in a well-ordered 2D hexagonal array.

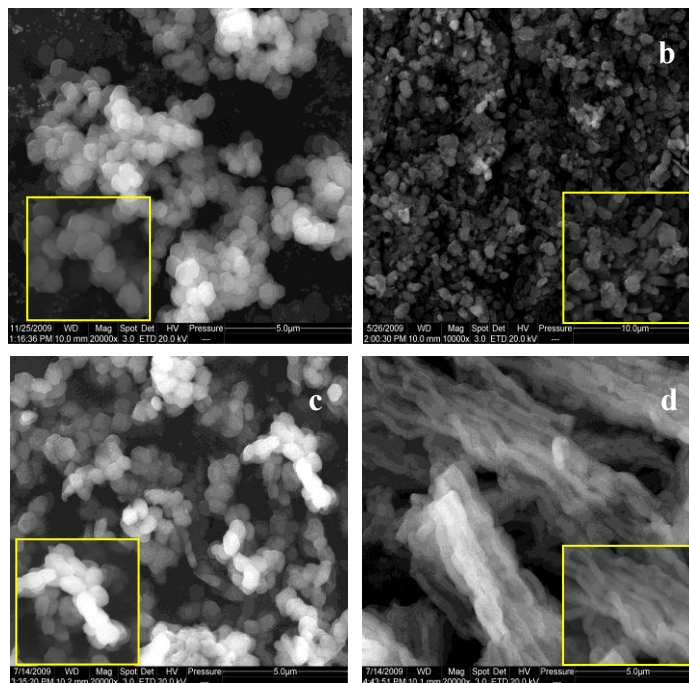


Fig. 1. SEM images of mesoporous SBA-15 silicas of (a) sample A, (b) sample B, (c) sample C and (d) sample D.

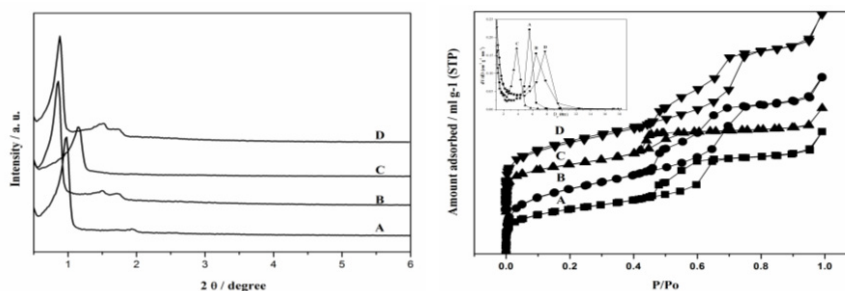


Fig. 2. (a) XRD patterns of sample A, B, C and D; (b) Nitrogen sorption isotherms of A, B, C and D materials.

Table 1. Porous properties and VOC adsorption performance of various samples.

Sample	N ₂ sorption				d ₁₀₀ (nm)	a _o (nm)	W (nm)	Dynamic capacity of toluene (ml/g)
	S _{BET} (m ² /g)	V _{total} (mL/g)	V _{micro} (mL/g)	D _p (nm)				
A	495	0.54	0.089	5.58	9.01	10.40	4.82	0.1931
B	715	0.77	0.122	6.47	10.26	11.85	5.38	0.2160
C	496	0.45	0.083	3.82	8.02	9.26	5.44	0.4158
D	644	0.81	0.094	7.72	9.81	11.32	3.60	0.3219
MCM-41	539	0.64	-	2.43	3.94	4	2.12	0.1521

3.2. Dynamic VOC Adsorption/Desorption Behavior

Breakthrough measurement is a direct method designed to clarify the dynamic performance of VOCs adsorption at low concentration. The dynamic adsorption behavior of C₇H₈ is evaluated on the mesoporous SBA-15 samples. The breakthrough curve of C sample has an exceptionally good shape, exhibiting a long breakthrough time (ca. 150 min) and a rapid increase after the breakthrough compared to other mesoporous SBA-15 materials. Sample A shows the second longest breakthrough time and a relatively rapid increase after breakthrough but plays the worst adsorption capacity. The adsorption capacity of B sample is much lower than that of sample C because of its shorter breakthrough time. The breakthrough time of D SBA-15 sample (about 60 min) is much shorter than that of C while it is still longer than that of A and B. Sample C has a rapid increase in the breakthrough curve, which means that it is little resistant to transfer mass in intraparticle. Therefore, the adsorption equilibrium is traced rapidly after the breakthrough. Fig. 3 (b) shows the desorption curves of the mesoporous SBA-15 samples. It can be noticed that sample C has the highest desorption amount corresponds to its high adsorption ability and the lowest temperature for the start of desorption and the complete elimination of toluene. It is illustrated that it is easier to remove toluene in contrast with other samples. The desorption behaviors of other samples are almost the same, indicating that the difference between their structure does not play an important role on their desorption performance. As is known that, the main channels of VOC removing from mesoporous silicas are the mesostructures.

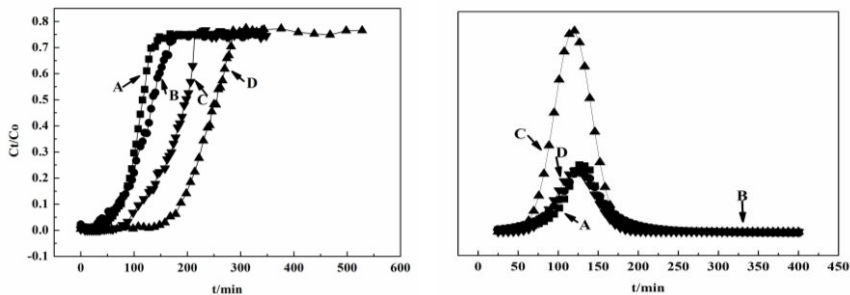


Fig. 3. The VOC breakthrough curves (a) and desorption curves (b) for four samples.

3.3. Effect of Pore Structure and Morphology on Dynamic Sorption Behavior

Fig. 4 depicts the relationship of the total pore volume - dynamic VOC capacities and micropore volume - dynamic VOC capacities for all SBA-15 samples. The figure shows that adsorbents with a larger volumetric capacity do not definitely have a larger breakthrough capacity. Only micropore volumes doesn't lead to a high adsorption capacity, either. Compared with the adsorption capacity of MCM-41 sample, it is indicated that the presence of micropores and the appropriate mesopore size directly lead to an increase in the dynamic capacity for these VOCs. Micropores are primarily responsible for the adsorption of gaseous molecules due to the overlap of attractive forces from opposing pore walls [14]. In the analysis, it is observed that the adsorption capacity of samples is concerned with not only the presence of microporosity but also the mesopore size. As the molecule diameter of toluene is about 0.60 nm, large pore size could contribute to the diffusion of but make it difficult to gather the molecules. The previous study has demonstrated that a decrease in the pore size of MCM-41 silicas from mesopores (3 nm) to micropores (1.35 nm) led to a dramatic increase in the dynamic adsorption performance. The macroscopic morphology also plays a great part in the adsorption process. The slower adsorption behavior of the fiberlike particles was the result of hindered diffusion [15]. Additionally, a rodlike SBA-15 100-200 nm in length with a larger mesopore size of 8-13 nm was recently reported to have exhibited a much faster adsorption rate in a similar reaction. It can be seen from the SEM images that rodlike particles are interconnected which increases the length of mesochannels, and have the least volume of micropores and the smallest size of the mesopore, so sample C performed the best adsorption capacity. It is suggested that the adsorption capacity of samples for VOC is concerned with both pore structures and morphology.

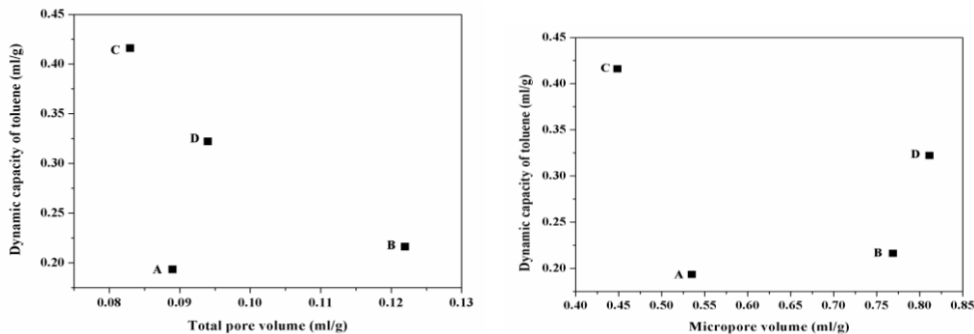


Fig. 4. Relationship between the total pore volume and dynamic VOC capacity (a), the micropore volume and dynamic VOC capacity (b) for A, B, C and D SBA-15 samples.

4. Conclusions

The dynamic VOC adsorption/desorption behaviors were evaluated for four kinds of SBA-15 silicas with different morphologies and distinct structural parameters. Both pore structural and morphological characteristics differ from each other, and these characteristics have proven to be important factors that affect the dynamic VOC adsorption/desorption properties of silica samples. The existence of micropores and the suitable mesopore size in the silica based adsorbents are essential contributory factors in achieving a large dynamic capacity. SBA-15 silicas with interconnected rodlike morphology and the appropriate 2D pore system appear to be suitable for use in a continuous adsorption-recycling system on the basis of both their large dynamic capacity and good desorption performance.

Acknowledgements

This work was supported financially by the Program for New Century Excellent Talents in University (NCET-09-0256) and the National Nature Science Foundation of China (No. 20807010).

References

- [1] Lei W, Zhang R, Tie X, Hess P. Chemical characterization of ozone formation in the Houston-Galveston area: A chemical transport model study. *J. Geophys. Res.* 2004;**109**: D12301.
- [2] Hu Q, Hao ZP, Li LD, Qiao SZ. Dynamic adsorption of volatile organic compounds on organofunctionalized SBA-15 materials. *Chem. Eng. J.* 2009;**149**:281-288.
- [3] Serrano DP, Calleja G, Botas JA, Gutierrez FJ. Adsorption and hydrophobic properties of mesostructured MCM-41 and SBA-15 materials for volatile organic compound removal. *Ind. Eng. Chem. Res.* 2004;**43**: 7010-7018.
- [4] Guillemot M, Mijoin J, Mignard S, Magnoux P. Adsorption of tetrachloroethylene on cationic X and Y zeolites: influence of cation nature and of water vapor. *Ind. Eng. Chem. Res.* 2007;**46**:4614-4620.
- [5] Kosuge K, Kubo S, Kikukawa N, Takemori M. Effect of pore Structure in mesoporous silicas on VOC dynamic adsorption/desorption performance. *Langmuir.* 2007;**23**:3095-3102.
- [6] Kruk M, Jaroniec M, Ko CH, Ryoo R.. Characterization of the porous structure of SBA-15. *Chem. Mater.* 2000;**12**:1961-1968 (b) Clere M I, Davidson P, Davidson A. Existence of a microporous corona around the mesopores of silica-based SBA-15 materials templated by triblock copolymers. *J. Am. Chem. Soc.* 2000;**122**:11925-11933.
- [7] Newalkar BL, Choudary NV, Turaga UT, Vijayalakshmi RP, Kumar P, Komarneni S, Bhat TSG. Potential adsorbent for light hydrocarbon separation: role of SBA-15 framework porosity. *Chem. Mater.* 2003;**15**:1474-1479.
- [8] Zhao D, Sun J, Li Q, Stucky GD. Morphological control of highly ordered mesoporous silica SBA-15. *Chem. Mater.* 2000;**12**:275-279.
- [9] Yu CZ, Fan J, Tian BZ, Zhao DY. Morphology development of mesoporous materials: a colloidal phase separation mechanism. *Chem. Mater.* 2004;**16**: 889-898.
- [10] Liu J, Li C, Yang Q, Yang J, Li C. Morphological and structural evolution of mesoporous silicas in a mild buffer solution and lysozyme adsorption. *Langmuir.* 2007;**23**:7255-7262.
- [11] Sujandi SE, Park DS, Han SC, Han MJ, Jin T. Ohsuna, Amino-functionalized SBA-15 type mesoporous silica having nanostructured hexagonal platelet morphology. *Chem. Commun.* 2006: 4131-4133.
- [12] Zhu YF, Shi JL, Shen WH, Dong XP, Feng JW, Ruan ML, Li YS. Stimuli-Responsive Controlled drug release from a hollow mesoporous silica sphere/polyelectrolyte multilayer core-shell structure. *Angew. Chem. Int. Ed.* 2005;**44**: 5083-5087.
- [13] Zhao DY, Huo QS, Feng JL, Chmelka BF, Stucky GD. Nonionic triblock and star diblock copolymer and oligomeric surfactant syntheses of highly ordered, hydrothermally stable, mesoporous silica structures. *J. Am. Chem. Soc.* 1998;**120**: 6024-6036.
- [14] Sing KSW, Everett DH, Haul RAW, Moscou L, Pierotti R A, Rouquerol J, Siemieniowska T. *Pure. Appl. Chem.* 1985;**57**:603-619.
- [15] Kosuge K, Sato T, Kikukawa T, Takemori M. Morphological Control of rod- and fiberlike SBA-15 type mesoporous silica using water-soluble sodium silicate. *Chem. Mater.* 2004;**16** (5):899-905